



Stability of fluorinated double-walled carbon nanotubes produced by different fluorination techniques

Lg Bulusheva, Yv Fedoseeva, Av Okotrub, E. Flahaut, Ip Asanov, Vo Koroteev, A. Yaya, Christopher Ewels, Al Chuvilin, A. Felten, et al.

► To cite this version:

Lg Bulusheva, Yv Fedoseeva, Av Okotrub, E. Flahaut, Ip Asanov, et al.. Stability of fluorinated double-walled carbon nanotubes produced by different fluorination techniques. Chemistry of Materials, 2010, 22 (14), pp.4197-4203. 10.1021/cm100677c . hal-00848930

HAL Id: hal-00848930

<https://hal.science/hal-00848930>

Submitted on 10 Dec 2021

HAL is a multi-disciplinary open access archive for the deposit and dissemination of scientific research documents, whether they are published or not. The documents may come from teaching and research institutions in France or abroad, or from public or private research centers.

L'archive ouverte pluridisciplinaire **HAL**, est destinée au dépôt et à la diffusion de documents scientifiques de niveau recherche, publiés ou non, émanant des établissements d'enseignement et de recherche français ou étrangers, des laboratoires publics ou privés.



Open Archive TOULOUSE Archive Ouverte (OATAO)

OATAO is an open access repository that collects the work of Toulouse researchers and makes it freely available over the web where possible.

This is an author-deposited version published in : <http://oatao.univ-toulouse.fr/>
Eprints ID : 4752

To link to this article : DOI :10.1021/cm100677c
URL : <http://dx.doi.org/10.1021/cm100677c>

To cite this version : Bulusheva, L. G. and Fedoseeva, Yu. V. and Okotrub, A. V. and Flahaut, Emmanuel and Asanov, I. P. and Koroteev, V. O. and Yaya, A. and Ewels, C. P. and Chuvilin, A. L. and Felten, A. and Van Lier, G. and Vyalikh, D. V. (2010) *Stability of fluorinated double-walled carbon nanotubes produced by different fluorination techniques*. Chemistry of Materials, vol. 22 (n° 14). pp. 4197-4203. ISSN 0897-4756

Any correspondence concerning this service should be sent to the repository administrator: staff-oatao@inp-toulouse.fr.

Stability of Fluorinated Double-Walled Carbon Nanotubes Produced by Different Fluorination Techniques

L. G. Bulusheva,^{*,†} Yu. V. Fedoseeva,[†] A. V. Okotrub,[†] E. Flahaut,^{‡,§} I. P. Asanov,[†]
V. O. Koroteev,[†] A. Yaya,^{||} C. P. Ewels,^{||} A. L. Chuvilin,^{⊥,⊗} A. Felten,[○]
G. Van Lier,[#] and D. V. Vyalikh[▽]

[†]Nikolaev Institute of Inorganic Chemistry, SB RAS, Novosibirsk, Russia, [‡]Centre Interuniversitaire de Recherche et d'Ingenierie des Materiaux, Universite Paul-Sabatier, France, [§]CNRS, Institut Carnot Cirimat, F-31062 Toulouse, France, ^{||}Institut des Materiaux Jean Rouxel, CNRS-Universite de Nantes, France, [⊥]CIC nanoGUNE Consolider, E-20018 San Sebastian, Spain, [⊗]IKERBASQUE, Basque Foundation for Science, Bilbao, Spain, [○]Laboratoire Interdisciplinaire de Spectroscopie Electronique, Facultes Universitaires Notre Dame de la Paix, Belgium, [#]Research Group of General Chemistry (ALGC), Vrije Universiteit Brussel – Free University of Brussels (VUB), Pleinlaan 2, B-1050, Brussels, Belgium, and [▽]Institute of Solid State Physics, Dresden University of Technology, D-01062 Dresden, Germany

Double-walled carbon nanotubes (DWCNTs) have been fluorinated using (1) gaseous F₂ at 200 °C, (2) a mixture of BrF₃ and Br₂ at room temperature, and (3) radio frequency CF₄ plasma. The stability of the resultant samples was examined by thermogravimetric analysis in an inert atmosphere and by comparing the X-ray photoelectron spectra of the pristine samples with those after heating in vacuum at either 70 °C for 10 h or 120 °C for 20 h. The DWCNTs fluorinated by F₂ showed the highest stability (the temperature of decomposition is around 396 °C), while the BrF₃ and plasma-fluorinated DWCNTs lose fluorine from 150 °C. Prolonged annealing of the fluorinated DWCNTs in vacuum at a temperature below 150 °C also resulted in the defluorination of the samples. Fluorine atoms leave the DWCNT surface together with carbon atoms leading to defects in the graphitic network. These defects are likely to be centers for later functionalization by oxygen-containing groups during DWCNT storage.

Introduction

Fluorination of the surface of carbon nanotubes (CNTs) creates new possibilities for the development of CNT derivatives, separation of nanotubes, and their application in various fields.¹ It has been shown that the addition of fluorine to the side walls of single-wall CNTs (SWCNT) significantly alters their electric conductivity, optical properties, and solubility.² Good solvation of fluorinated SWCNTs in alcohols³ allows one to make further chemistry⁴ and to disperse nanotubes in a polymer matrix.⁵ Use for this purpose of double-walled CNTs (DWCNTs) is of special interest because only the surface of the external CNT is fluorinated, while the internal CNT preserves its own unique

electronic and optical characteristics.^{6,7} As a result, the use of fluorinated DWCNTs is promising for reinforcement of polymer composites as well as in electronics and sensor applications.

One of the advantages of fluorination is the possibility to recover the CNT surface by treatment with hydrazine^{3,8} or heating the fluorinated sample in an inert atmosphere.⁹ Annealing of fluorinated SWCNTs at 100 °C during 1 h in argon or helium flow was shown to activate the vibrations of the graphitic network of CNTs in the IR-region.⁹ Analysis of Raman data indicated that thermal defluorination results in conversion of most of the fluorinated SWCNTs back to the initial state; however, a part of the CNTs is etched with the creation of defects and/or amorphous carbon phases.¹⁰ The IR-spectroscopic study of argon matrix isolated products of the thermal decomposition of fluorinated SWCNTs found that fluorine atoms leave the CNT surface together with carbon atoms.¹¹ The main detected species are COF₂ below 300 °C and CF₄ at

*To whom correspondence should be addressed. E-mail: bul@niic.nsc.ru.

(1) Lee, Y.-S. *J. Fluor. Chem.* **2007**, 128, 392.

(2) Khabashesku, V. N.; Billups, W. E.; Margrave, J. L. *Acc. Chem. Res.* **2002**, 35, 1087.

(3) Mickelson, E. T.; Chiang, I. W.; Zimmerman, J. L.; Boul, P. J.; Lozano, J.; Liu, J.; Smalley, R. E.; Hauge, R. H.; Margrave, J. L. *J. Phys. Chem. B* **1999**, 103, 4318.

(4) Pulikkathara, M. X.; Khabashesku, V. N. *Chem. Mater.* **2008**, 20, 2685.

(5) Miyagawa, H.; Drzal, L. T. *Polymer* **2004**, 45, 5163.

(6) Muramatsu, H.; Kim, Y. A.; Hayashi, T.; Endo, M.; Yonemoto, A.; Arikai, H.; Okino, F.; Touhara, H. *Chem. Commun.* **2005**, 2002.

(7) Hayashi, T.; Shimamoto, D.; Kim, Y. A.; Muramatsu, H.; Okino, F.; Touhara, H.; Shimada, T.; Miyauchi, Y.; Maruyama, S.; Terrones, M.; Dresselhaus, M. S.; Endo, M. *ACS Nano* **2008**, 2, 485.

(8) Marcoux, P. R.; Schreiber, J.; Batail, P.; Lefrant, S.; Renouard, J.; Jacob, G.; Albertini, D.; Mevellec, J.-Y. *Phys. Chem. Chem. Phys.* **2002**, 4, 2278.

(9) Zhao, W.; Song, C.; Zheng, B.; Liu, J.; Viswanathan, T. *J. Phys. Chem. B* **2002**, 106, 293.

(10) Pehrsson, P. E.; Zhao, W.; Baldwin, J. W.; Song, C.; Liu, J.; Kooi, S.; Zheng, B. *J. Phys. Chem. B* **2003**, 107, 5690.

(11) Bettinger, H. F.; Peng, H. *J. Phys. Chem. B* **2005**, 109, 23218.

higher annealing temperatures. X-ray photoelectron spectroscopy (XPS) showed that annealing of the fluorinated DWCNTs at 300 °C in vacuum conditions removed most of the fluorine atoms, while the electronic state of carbon in the product was different from that in the pristine non-fluorinated sample.¹²

There are several ways to fluorinate CNTs, the most common being fluorination by F₂ at elevated temperatures,¹³ by gaseous BrF₃ at room temperature,¹⁴ and using a treatment with CF₄ plasma.¹⁵ The first method yields the highest fluorination degree to the CNT surface with a C₂F composition for SWCNTs, while the limiting composition achieved using the second method is C₃F. For plasma treated multiwalled CNTs (MWCNTs), the surface fluorine concentration can be controlled by the reaction time and plasma power up to C₂F.^{16,17} The differences in fluorination conditions, particularly in the kinetic energy of the fluorinating agent, should result in different surface reaction mechanisms and consequently in various fluorine patterns on the CNT surface, which will ultimately determine the specific properties and possible applications of the fluorinated material.^{18,19}

In the present work we compare the thermal stability of fluorinated DWCNTs produced using the three above-mentioned fluorination methods with that of purified DWCNTs taken from the same batch. The thermal decomposition of pristine and fluorinated samples in an argon atmosphere was studied by thermogravimetric analysis (TGA). The electronic state of carbon and fluorine in the samples, subjected to prolonged heating at fixed temperature in vacuum, was examined by near edge X-ray absorption fine structure (NEXAFS) spectroscopy. The composition of the fluorinated DWCNTs and those after annealing and storage in a laboratory environment was determined by XPS.

Method

DWCNTs were produced by decomposition of CH₄ vapor (CCVD, catalytic chemical vapor deposition method) over Mg_{1-x}Co_xO solid solution containing small additions of molybdenum.²⁰ High-resolution transmission electron microscopy showed that a typical sample

consists of about 80% DWCNTs, 15% SWCNTs, and a small amount of triple-walled nanotubes. The diameter distribution of the DWCNTs ranged from 0.5 to 2.5 nm for the inner tubes and from 1.2 to 3.2 nm for the outer tubes. DWCNTs were purified by a procedure described elsewhere.²¹ Briefly, the sample was heated in air at 450 °C for 1 h followed by treatment with concentrated HCl (37%) to dissolve metal oxides formed during the oxidation process, and then washed with deionized water and dried at 30 °C in vacuum.

The 0.7 nm difference between the inner and outer nanotube diameter corresponds in general to a (*n*+9,*m*) helicity for the outer tube for a (*n*,*m*) inner nanotube.²² Given a Gaussian distribution of the diameters, based on the experimentally observed diameter distribution²⁰ the mean inner diameter is 1.5 nm. We therefore take as a mean DWCNT an inner (19,0) zigzag nanotube (diameter 1.489 nm), and a (28,0) outer nanotube (diameter 2.193 nm) when calculating the fluorine relative atomic concentrations below.

Fluorination of DWCNTs using fluorine gas was conducted at 200 °C for 10 min. F₂ gas was produced by electrolysis of liquid anhydrous HF and not purified to remove HF traces, expected to act as a catalyst. Fluorination by gaseous BrF₃ was carried out in a Teflon flask, where the sample was held over a solution of Br₂ and BrF₃ for 7 days. Dilution of BrF₃ by bromine decreases the reaction rate, lowering the amount of the released energy. The flask content was then dried by a flow of N₂ until no more Br₂ was released (~48 h). Plasma fluorination was performed by exposing DWCNTs to a CF₄ plasma for 10 min (full methodology is described in refs 16,17). Plasma frequency and power were 13.56 MHz and 15 W respectively, and the chamber pressure was 0.1 Torr. The nanotubes were not stirred or agitated during the process.

The TGA study was performed with a SETARAM TAG24 thermobalance. In the TGA experiments, the sample was heated in an argon atmosphere from 25 to 600 °C continuously. The heating rate was 1 °C/min.

The NEXAFS experiments were carried out at the Berliner Elektronenspeicherring für Synchrotronstrahlung (BESSY) using radiation from the Russian-German beamline. NEXAFS spectra near the C K- and F K-edges were acquired in the total-electron yield mode with a typical probing depth of a few nanometers.²³ The spectra were normalized to the primary photon current from a gold-covered grid recorded simultaneously. The monochromatization of the incident radiation was ~80 meV in the carbon absorption region and ~170 meV in the fluorine absorption region, both full width at half-maximum (fwhm). The samples were annealed at 70 °C for 12 h and at 120 °C for 20 h in vacuum chamber before the experiments.

The overall XPS of the initial DWCNTs, fluorinated DWCNTs and the annealed fluorinated samples were

- (12) Bulusheva, L. G.; Gevko, P. N.; Okotrub, A. V.; Lavskaya, Yu. V.; Yudanov, N. F.; Yudanov, L. I.; Abrosimov, O. G.; Pazhetnov, E. M.; Boronin, A. I.; Flahaut, E. *Chem. Mater.* **2006**, *18*, 4967.
- (13) Mickelson, E. T.; Huffman, C. B.; Rinzler, A. G.; Smalley, R. E.; Hauge, R. H.; Margrave, J. L. *Chem. Phys. Lett.* **1998**, *296*, 188.
- (14) Gevko, P. N.; Bulusheva, L. G.; Okotrub, A. V.; Yudanov, N. F.; Yushina, I. V.; Grachev, K. A.; Pugachev, A. M.; Surovtsev, N. V.; Flahaut, E. *Fullerenes, Nanotubes, Carbon Nanostruct.* **2006**, *14*, 233.
- (15) Felten, A.; Chijsen, J.; Pireaux, J.-J.; Johnson, J.-J.; Whelan, C. M.; Liang, D.; Van Tendeloo, G.; Bittencourt, C. *Carbon* **2008**, *46*, 2171.
- (16) Felten, A.; Bittencourt, C.; Van Lier, G.; Charlier, J.-C.; Pireaux, J. J. *J. Appl. Phys.* **2005**, *98*, 074308.
- (17) Bittencourt, C.; Van Lier, G.; Ke, X.; Martinez-Suarez, I.; Felten, A.; Ghijsen, J.; Van Tendeloo, G.; Ewels, C. P. *Chem. Phys. Chem.* **2009**, *10*, 920.
- (18) Ewels, C. P.; Van Lier, G.; Charlier, J.-C.; Heggie, M. I.; Briddon, P. R. *Phys. Rev. Lett.* **2006**, *96*, 216103.
- (19) Osuna, S.; Torrent-Sucarrat, M.; Solà, M.; Geerlings, P.; Ewels, C. P.; Van Lier, G. *J. Phys. Chem. C* **2010**, *114*, 3340.
- (20) Flahaut, E.; Bacsá, R.; Peigney, A.; Laurent, Ch. *Chem. Commun.* **2003**, 1442.

(21) Osswald, S.; Flahaut, E.; Gogotsi, Y. *Chem. Mater.* **2006**, *18*, 1525.

(22) Guo, W.; Guo, Y. *J. Am. Chem. Soc.* **2007**, *129*, 2730.

(23) Stöhr, J. *NEXAFS spectroscopy*; Springer Verlag: Berlin, 1992;

recorded on a SpecsLab PHOIBOS 150 spectrometer. The spectra were excited with monochromatic X-ray emission Al K α (1486.6 eV). The measurements of the annealed samples were carried out after keeping the samples in laboratory conditions for half a year. The base pressure in the spectrometer chamber during experiments was 10^{-9} mbar.

The transmission electron microscopy (TEM) study was performed using a Titan 80–300 image side Cs-corrected electron microscope (FEI, Netherlands) at 80 kV accelerating voltage.

Theoretical spin polarized density functional theory (DFT) calculations were performed using the AIMPRO code,^{24,25} on an orthorhombic 32 atom supercell of graphene using a $2 \times 2 \times 2$ k-point grid. Hartwigsen–Goedecker–Hutter relativistic pseudopotentials²⁶ were used for all atoms. Atom-centered Gaussian basis functions were used to construct the many-electron wave function with angular momenta up to $l = 2$. Electronic level occupation was obtained using a Fermi occupation function with $kT = 0.04$ eV.

Results and Discussion

The TG investigation of the samples revealed that the process of decomposition of fluorinated DWCNTs is different from that of the pristine nanotubes and results in different products depending on the fluorination techniques (Figure 1a). The differential TG (DTG) curves show that the weight loss of pristine DWCNTs starts from about 450 °C, and the sample then loses weight continuously with increasing temperature (curve 4 in Figure 1b). The F₂ fluorinated DWCNTs are stable up to 100 °C, and most of the fluorine atoms are detached from the nanotube surface in the interval from 250 to 475 °C with a minimum in the DTG curve at about 395 °C (curve 1 in Figure 1b). The weight of the sample fluorinated by BrF₃ begins to decrease below 100 °C (curve 2 in Figure 1b), which can be attributed to removal of bromine molecules trapped in the intertube space. The fluorine atoms are removed from the sample mainly at temperatures from 250 to 455 °C. The plasma-treated DWCNTs gradually lose weight starting from 100 °C (curve 3 in Figure 1b). The DTG curves for all the fluorinated DWCNTs have a minimum around 585 °C that could be due to destruction of the CNT cage. Interestingly, fluorine removal from the fluorinated DWCNTs produced by different methods occurs in different temperature intervals, indicative of different binding energy of fluorine atoms with the DWCNT surface.

The overall XPS spectra of the fluorinated samples show signals of carbon, fluorine, and oxygen. The concentration of elements in the samples was estimated from the ratio of the areas of the corresponding lines taking into account the photoionization cross sections (see Table 1).

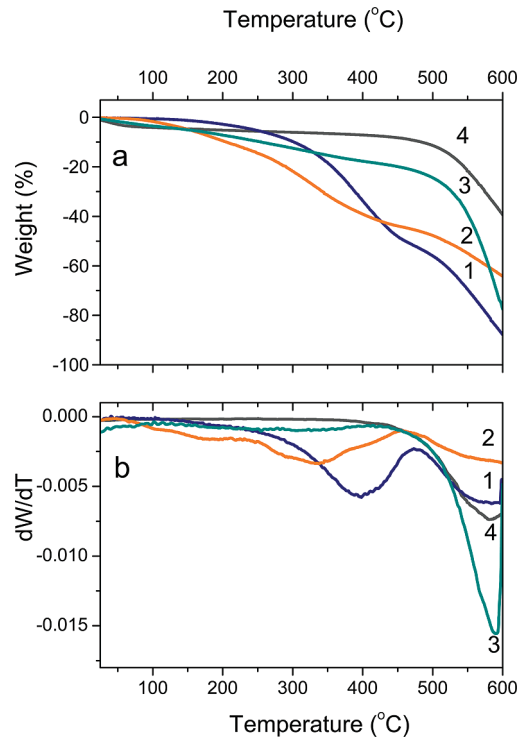


Figure 1. Thermal gravimetric (TG) (a) and differential TG (DTG) (b) curves for DWCNTs fluorinated by F₂ (1), BrF₃ (2), and with CF₄ plasma (3) and for pristine non-fluorinated DWCNTs (4).

The DWCNTs fluorinated by a mixture of BrF₃ and Br₂ additionally contained ~1 at % of bromine that was not considered in the following discussion. The highest concentration of fluorine was found in the sample fluorinated by F₂ at elevated temperature with a relative fluorine concentration of 20.30 at %. High-resolution TEM investigation of the sample indicated that the double-walled structure of nanotubes after F₂ action is preserved (Figure 2). The fluorine concentration in the samples fluorinated using BrF₃ and CF₄ plasma is equal to 13.80 at % and 11.06 at %, respectively.

We note that the relative atomic concentrations as determined by XPS include contributions of photoelectrons belonging to both walls of the DWCNTs. Nonetheless, the relative atomic concentration for fluorine only corresponds to outer wall functionalization. Since the nanotubes under consideration here are relatively small, there is a larger discrepancy between the amount of nanotubes per 1D unit cell for the inner and outer walls. The relative fluorine atomic concentrations given in Table 1 are therefore recalculated for the actual CF_x ratio on the outer wall given a mean nanotube of (19,0)@-(28,0) helicity (see above). This corresponds to a C/F ratio of 2.256, 3.643, and 4.746, thus giving approximate CF_{0.44}, CF_{0.27}, and CF_{0.21} addition ratios respectively for nanotubes treated by F₂, BrF₃, and CF₄ plasma (see Table 1). These values are close to the compositions of the fluorinated SWCNTs obtained in similar conditions.^{8,10,14,27} The limiting surface C/F ratio expected for certain fluorination

(24) Rayson, M. J.; Briddon, P. R. *Comput. Phys. Commun.* **2007**, *178*, 128.

(25) Briddon, P. R.; Jones, R. *Phys. Status Solidi B* **2000**, *217*, 131.

(26) Hartwigsen, C.; Goedecker, S.; Hutter, J. *Phys. Rev. B* **1998**, *58*, 3641.

(27) Plank, N. O. V.; Jiang, L.; Cheung, R. *Appl. Phys. Lett.* **2003**, *83*, 2426.

Table 1. Relative Atomic Concentration (at %) for Main Elements in the DWCNT Samples, Fluorinated by Different Fluorinating Agents, Evaluated by XPS, Together with the Weight Percentage (wt %) Given in Parenthesis, and Estimated CF_x Ratio for the Outer Nanotube of DWCNT (See Text)

F-DWCNT	carbon	fluorine	oxygen	bromine	CF_x surface ratio ^a
F ₂	75.24 (66.39)	20.30 (28.36)	4.46 (5.25)		0.44
BrF ₃	82.58 (72.06)	13.80 (19.07)	2.63 (3.06)	0.99 (5.82)	0.27
CF ₄	86.23 (80.32)	11.06 (16.31)	2.71 (3.37)		0.21

^a We note that the CF_x ratios estimated above are for a (19,0)@(28,0) nanotube. If the experimentally observed range of nanotube diameters is taken into account, namely from 0.5 to 2.5 nm for the inner tube, this gives ratios in the range of $CF_{0.37-0.48}$, $CF_{0.23-0.30}$ and $CF_{0.18-0.23}$ respectively.

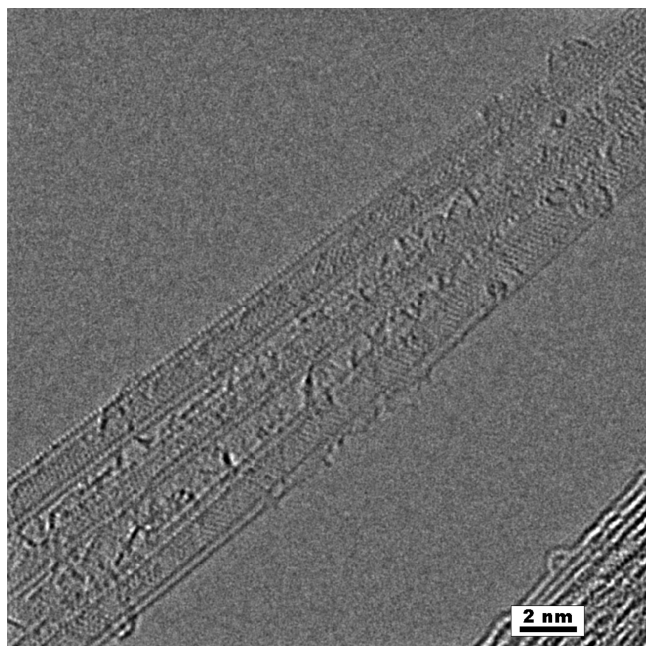


Figure 2. High resolution TEM image of DWCNTs fluorinated by F₂ at 200 °C.

methods is difficult to achieve for SWCNTs and DWCNTs because they usually form bundles. Fluorinating agents first act on the bundle surface and after that the kinetics of the fluorination process becomes considerably restricted because of the necessity for reagent penetration through the fluorinated layer. Even after repeated F₂ treatment at optimal conditions the SWCNTs were not completely dispersed.²⁸ TEM analysis of our fluorinated DWCNTs shows that average diameter of bundles in the sample fluorinated by CF₄ plasma is nearly the same as that in the pristine sample (~20 nm), while it decreases to ~12 nm and ~8 nm for the samples fluorinated by BrF₃ and F₂. The higher fluorination rate and deeper fluorine penetration provided by the F₂ gas method compared to the CF₄ plasma method have been previously observed by XPS for graphitized carbon materials.^{29,30} The plasma-enhanced fluorination is therefore assumed to form a thin fluorinated layer which does not affect the bulk properties of the material.

The concentration of oxygen is higher for the sample with the larger fluorine content (Table 1). The XPS examination of the pristine DWCNTs found ~2 at % of oxygen, which will be present as functional groups on the nanotube surface. These groups result from the purification procedure as well as from the storage of the CNTs in laboratory air. Fluorination of CNTs increases the amount of attached oxygen, as previously mentioned in ref 31. The increase in oxygen content in the fluorinated CNTs can result from fluorination in an air-containing atmosphere, which promotes the attachment of oxygen species to carbon atoms located near to fluorinated carbon atoms and thus having an additional charge. Also, fluorinated DWCNTs kept in ambient conditions could interact with oxygen-containing molecules leading to the substitution of fluorine atoms by hydroxyl groups. An XPS study of the functional sidewall composition of MWCNTs fluorinated by fluorine gas in an inert atmosphere revealed that the component ratio of the O 1s peak of fluorinated MWCNTs was almost the same as that of raw MWCNTs.³² Thus, we conclude that the increase of oxygen in our products more likely occurs during the fluorination procedure. The enhanced oxygen content in the DWCNTs fluorinated by F₂ could be due to the elevated temperature in the reactor. Moreover, the repeated XPS examination of the F₂ fluorinated DWCNTs after 1 year storage detected no change in sample composition, suggesting a slow rate of hydrolysis for such systems.

To provide a high vacuum (~10⁻⁹ mbar) during the NEXAFS experiments the holder with deposited samples has been annealed at 120 °C for 20 h. The spectra of the pristine and fluorinated DWCNT samples measured near the C K- and F K-edges are compared in Figure 3. The F K-edge NEXAFS spectra of the fluorinated samples have been aligned with the C K-edge spectra using the XPS data on the C 1s and F 1s binding energies. Intensity in the carbon region and fluorine region was normalized to the values at 330 eV (not shown in the Figure) and 711 eV, respectively. The C K-edge NEXAFS spectrum of the pristine DWCNTs exhibits two sharp resonances at ~284.5 and 291.5 eV corresponding to the 1s→π* and 1s→σ* transitions.³³ The splitting of the σ* resonance is indicative of the high graphitization level³⁴ of the DWCNTs. Fluorination of the sample causes a reduction

- (28) Krestinin, A. V. A.; Kharitonov, P.; Shul'ga, Yu. M.; Zhigalina, O. M.; Knerel'man, E. I.; Dubois, M.; Brzhezinskaya, M. M.; Vinogradov, A. S.; Preobrazhenskii, A. B.; Zvereva, G. I.; Kislov, M. B.; Martynenko, V. M.; Korobov, I. I.; Davydova, G. I.; Zhigalina, V. G.; Kiselev, N. A. *Nanotechnol. Russ.* **2009**, *4*, 60.
 (29) Tressaudt, A.; Moguet, F.; Flandroiss, S.; Chambon, M.; Guimon, C.; Nanset, G.; Papireri, E.; Gupta, V.; Bahl, O. P. *J. Phys. Chem. Solids* **1996**, *57*, 745.
 (30) Tressaud, A.; Durand, E.; Labrugère, Ch. *J. Fluor. Chem.* **2004**, *125*, 1639.

- (31) Wang, Y.-Q.; Sherwood, P. M. A. *Chem. Mater.* **2004**, *16*, 5427.
 (32) Lee, J.-M.; Kim, S. J.; Kim, J. W.; Kang, P. H.; Nho, Y. C.; Lee, Y.-S. *J. Ind. Eng. Chem.* **2009**, *15*, 66.
 (33) Li, Z.; Zhang, L.; Resasco, D. E.; Mun, B. S.; Requejo, F. G. *Appl. Phys. Lett.* **2007**, *90*, 103115.
 (34) Wessely, O.; Katsnelson, M. I.; Eriksson, O. *Phys. Rev. Lett.* **2005**, *94*, 167401.

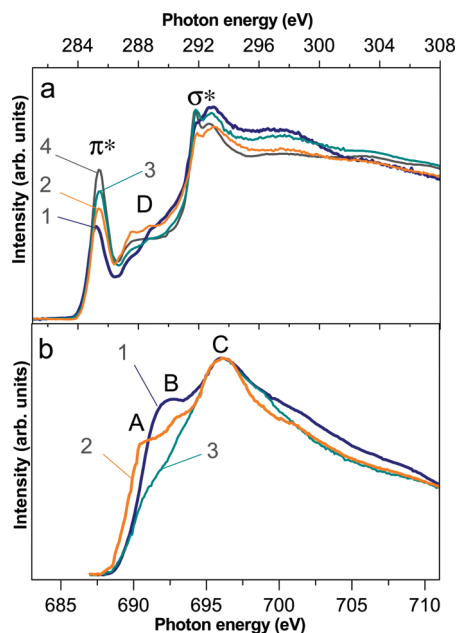


Figure 3. NEXAFS spectra measured near the C K-edge (a) and F K-edge (b) of DWCNTs fluorinated by F₂ (1), BrF₃ (2), and with CF₄ plasma (3) and for pristine non-fluorinated DWCNTs (4).

in the π^* resonance intensity, broadening of the σ^* resonance, and appearance of intensity between 287 and 289 eV labeled by D (Figure 3a). The relative intensity of the π^* resonance decreases with the increase of fluorine content in the DWCNT sample, demonstrating formation of covalent C–F bonds.

The F K-edge NEXAFS spectra of the fluorinated DWCNTs have an intense peak at 696 eV corresponding to the σ^* resonance (labeled C in Figure 3b) and pre-edge features, whose position and relative intensity are different for the samples produced by different methods. The coincidence of the pre-edge features of the F K-edge NEXAFS spectra with the D feature in the C K-edge spectra (after energy alignment of the spectra) indicates that the latter feature corresponds to the $1s \rightarrow \sigma^*$ transitions within carbon atoms bonded with fluorine. The variations in shape of the D feature could be due to different local surroundings of CF units on the CNT surface fluorinated in different conditions. This conclusion is supported by the large difference in the pre-edge structure of the F K-edge NEXAFS spectra of the samples. The spectrum of the DWCNTs fluorinated by F₂ (curve 1 in Figure 3b) shows a single intense peak B before the σ^* resonance. The pre-edge feature in the spectrum of the DWCNTs fluorinated by BrF₃ (curve 2 in Figure 3b) is split into two peaks A and B located at 690.7 and 693.2 eV, while the spectrum of plasma-treated DWCNTs has a shoulder at the low-energy side of the main peak (curve 3 in Figure 3b). We found only one paper presenting an F K-edge NEXAFS spectrum of fluorinated CNTs.³⁵ In this paper the MWCNTs were fluorinated by molecular fluorine at 420 °C, and the spectrum is closest to our

spectrum of fluorinated DWCNTs produced by the similar procedure. The F K-edge NEXAFS spectrum of the DWCNTs fluorinated by BrF₃ is akin to those of the SWCNTs and few-walled CNTs fluorinated in the same conditions.³⁶ It is likely that the fluorine pattern on the CNT surface is strongly determined by the fluorination method used.

Quantum-chemical calculations have previously indicated that the lowest energy configurations of fluorine atoms on CNT surfaces are (1,2) and (1,4) additions, where a second fluorine atom is attached in the *ortho*- and *para*- position respectively of a carbon hexagon.³⁷ For the C₂F and C₄F composition corresponding to the surface coverage of DWCNTs fluorinated by F₂ and BrF₃, these configurations lead to formation of alternated fluorocarbon and bare chains in the first structure and benzenoid rings surrounded by *para*-fluorinated hexagons in the second structure.¹⁸ The calculated binding energies per fluorine atom for C₂F and C₄F are 1.83 and 1.75 eV, in agreement with the highest stability of the F₂ fluorinated DWCNTs found from TGA analysis. It should be mentioned that the actual fluorine pattern in the investigated samples will be determined not only by the thermodynamic conditions but also the choice of fluorinating agent.

The surface composition of the fluorinated DWCNT samples annealed at 120 °C during 20 h or at 70 °C during 12 h in vacuum, and then kept in the laboratory atmosphere more than half a year was probed by XPS. Dependence of fluorine and oxygen concentration in the samples on the heating temperature is presented in Figure 4. One can see that the annealing resulted in partial defluorination of the DWCNTs (Figure 4a). The fluorine content in the samples fluorinated by F₂ and BrF₃ continuously decreases with increasing temperature and annealing time and at 120 °C annealing for 20 h, about half of the fluorine atoms are removed from the DWCNTs. The plasma-fluorinated sample loses two-third of its fluorine at 70 °C, and the stronger annealing conditions cause almost no further change in the sample content. Although the TG and DTG analysis showed negligible weight loss of the fluorinated DWCNTs at 70 and 120 °C, the XPS data indicate that with prolonged annealing at these temperatures the fluorine concentration in the samples is markedly decreased. This suggests that kinetics of species on the nanotube surface may play an important role.

It is interesting that oxygen content in the annealed fluorinated samples is much higher than in the as-prepared fluorinated samples (Figure 4b). Removal of fluorine atoms together with carbon atoms from CNT walls¹¹ will produce vacancies and edge sites. The carbon atoms constituting these defects have a higher reactivity toward the oxygen-containing molecules present in air. Quantum-chemical calculations have shown that the dissociation probability of water increases with an increase in the

(35) Brzhezinskaya, M. M.; Muradyan, V. E.; Vinogradov, N. A.; Preobrajenski, N. A.; Gudat, W.; Vinogradov, A. S. *Phys. Rev. B* **2009**, 79, 155439.

(36) Lavskaya, Yu. V.; Bulusheva, L. G.; Okotrub, A. V.; Yudanov, N. F.; Vyalikh, N. F.; Fonseca, A. *Carbon* **2009**, 47, 1629.

(37) Bettinger, H. F. *ChemPhysChem* **2003**, 4, 1283.

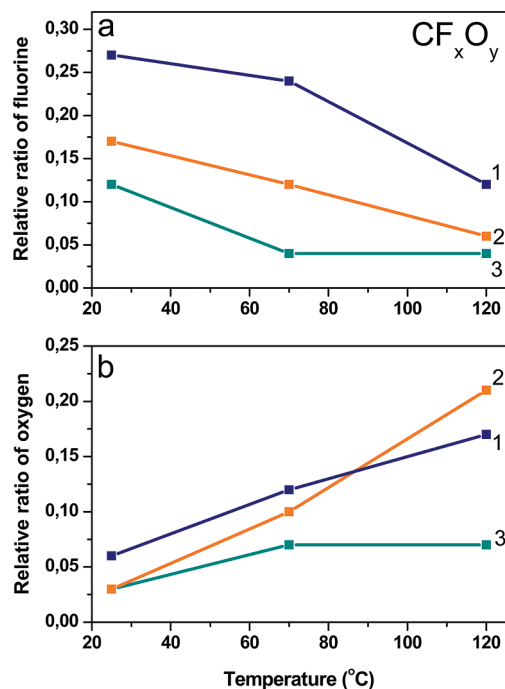


Figure 4. Concentration of fluorine (a) and oxygen (b) in the DWCNTs fluorinated by F₂ (1), BrF₃ (2), and with CF₄ plasma (3) as a function of the annealing temperature.

number of structural defect sites on the graphite sheet.³⁸ The proposition, that annealing of the fluorinated DWCNTs results in etching of nanotube shells, is supported by analysis of the TGA data (Figure 1). The data shows that the weight loss of the sample fluorinated by F₂ (BrF₃) is 52 wt % (44 wt %) at 473 °C (455 °C) when removal of the fluorine atoms is complete. Taking into account the concentration of elements determined by XPS (table 1), assuming the DWCNTs fluorinated by F₂ and BrF₃ lose all their fluorine, oxygen, and bromine atoms (for the latter sample), to account for the observed weight loss they must also lose respectively 18 wt % and 16 wt % of carbon atoms. Considering that the internal shells of the DWCNTs were not fluorinated, this implies that the loss of carbon corresponds to losing about 46% and 36% of the external shells. This result agrees with TGA investigations of fluorinated SWCNTs with composition CF_{0.2}, which detected ~45% overall weight loss of the sample.³⁹ Because fluorine atoms are removed as COF₂ and CF₄ species,^{11,39} additional oxygen atoms, which are needed to provide weight balance, can originate from impurities in the argon used in the TGA experiment and/or from molecules adsorbed on the DWCNT surface. Unlike the other samples, the loss of the plasma-fluorinated DWCNT sample heated up to 437 °C is 20 wt %, which corresponds to the complete removal of all fluorine and oxygen atoms and less than 1 at % of the carbon. This amount of carbon is insufficient to bind all fluorine and oxygen atoms in the molecular species. However, if fluorine is concentrated on the surface of large-size DWCNT bundles, the XPS will overestimate the F/C ratio

for the plasma-fluorinated sample. In any case it appears that the decomposition of this sample results in the formation of fluorocarbon molecules but with considerably less destruction of CNT walls than for the samples fluorinated by F₂ and BrF₃.

Comparison of the XPS and TGA results indicates that stability of the fluorinated DWCNTs depends on the method of fluorination. Thermal defluorination results in partial etching of the walls in DWCNTs fluorinated by F₂ and BrF₃ and has almost no destructive effect on the DWCNTs fluorinated with CF₄ plasma. We can speculate briefly about possible origins for the different behavior observed in the plasma treated samples. In the CF₄ plasma, molecular fragments are produced, not only F but also CF_x (x = 1–3). Indeed, the XPS C 1 spectrum of plasma fluorinated DWCNTs showed the peaks corresponding to CF₂ and CF₃ groups. Attachment of large moieties such as CF₂ and CF₃ to the nanotube surface could obstruct further surface fluorination, restricting the maximum attainable fluorine surface concentration as observed. Additionally if weakly surface mobile at 70 °C, it is feasible that they could migrate and combine with other surface species (F, CF_x), leading to the observed kinetically limited weight loss in the sample in this temperature range. Loss of surface material in this way would not involve loss of carbon from the nanotube wall, consistent with the “pristine-like” tube stability seen in TGA data and the constant oxygen levels in the sample determined from XPS.

To investigate this model for CF₄-plasma treated tubes we performed DFT calculations of both single F and CF_x attachment to a graphene surface. Binding energies are calculated relative to an isolated relaxed perfect graphene sheet, and a single isolated molecular fragment (F, CF₂, CF₃). F atom binds with 2.37 eV, whereas the binding energy of CF₂ and CF₃ groups is 1.04, and 0.90 eV per fragment, respectively, with the former having carbene-like addition. Sequential detachment of the CF_x moieties with heating temperature could explain continuous weight loss of the plasma fluorinated DWCNTs beginning from 100 °C. Moreover, the weakly bound CF₃ could surface migrate until collecting either F to release CF₄ or another CF₃ to release C₂F₆. Assuming Arrhenius-like kinetics behavior, with attempt frequency of 10¹³ Hz (Debye frequency), at 70 °C CF₃ will be making 9.4 hops/second while F will be immobile. It also suggests that plasma treatment time may strongly influence surface composition, since such surface kinetics will presumably also be important for initial covering.

Conclusion

Three different methods have been used for the fluorination of CVD-produced DWCNTs. The thermal stability of the products was studied using TG and DTG analysis; additionally the surface chemical composition of the long-time annealed fluorinated DWCNTs was determined by XPS. The thermal defluorination process was found to depend strongly on the method of DWCNT fluorination. Increase in the temperature and duration of

(38) Zhanpeisov, N. U.; Zhidomirov, G. M.; Fukumura, H. *J. Phys. Chem. C* **2009**, *113*, 6118.

(39) Gu, Z.; Peng, Z.; Hauge, R. H.; Smalley, R. E.; Margrave, J. L. *Nano Lett.* **2002**, *2*, 1009.

sample annealing in vacuum results in progressive removal of fluorine from DWCNTs fluorinated by F_2 or BrF_3 . The fluorine atoms withdraw together with carbon atoms, creating vacancies and edge-sites. The defect sites may promote dissociation of water molecules and development of oxygen-containing groups on the surface of the annealed fluorinated DWCNTs kept in a laboratory atmosphere. DWCNTs fluorinated with CF_4 plasma lose most of their fluorine after sample annealing at 70 °C during 12 h, with negligible etching of CNT walls. The different stability of the fluorinated DWCNTs produced by different methods demonstrates different binding energy between carbon and fluorine atoms that is likely due to the various mechanisms of nanotube fluorination. Our

calculations support a model whereby F_2 and BrF_3 fluorination proceed through direct fluorine addition to the nanotube exterior, while CF_4 plasma fluorination adds a mix of species including F, CF_2 , and CF_3 .

Acknowledgment. The work was supported by the bilateral Program “Russian-German Laboratory at BESSY, the French Embassy in Russia, and the COST project NanoTP. We are grateful to Dr. M.M. Brzhezinskaya for technical support during the experiments at BESSY. G.V.L. acknowledges the Research Foundation-Flanders (FWO) for financial support as a Postdoctoral Research Fellow. C.P.E. and G.V.L. also acknowledge funding for scientific exchange between France and the Belgian Flemish community through the TOURNESOL 2009 Project T2009.19.